

## Polymerization of Acrylamide N-methylene Lactic and Glycolic Acid

Sevara Khazratkulova<sup>1</sup>  , Nodira Zokirova<sup>1</sup>  , Busora Mukhamedova<sup>1</sup>  , Basant Lal<sup>2</sup>  , Orifjon Khamidov<sup>3</sup>  , Elyor Berdimurodov<sup>\*4,5,6</sup>  , Guloy Alieva<sup>6</sup>  , Ahmad Hosseini-Bandegharai<sup>7</sup>  , Nizomiddin Aliev<sup>8</sup>  

<sup>1</sup>Faculty of Pharmacy, Tashkent Pharmaceutical Institute, Tashkent, Uzbekistan.

<sup>2</sup>Department of Chemistry, Institute of Applied Science and Humanities, University of GLA, Mathura-281406, India.

<sup>3</sup>Faculty of chemical technology, Navoi State University of Mining and Technologies, Navoiy, Uzbekistan.

<sup>4</sup>Chemical & Materials Engineering, New Uzbekistan University, 1, Movarounnahr street, Mirzo-Ulug'bek district, Tashkent, 100000, Uzbekistan.

<sup>5</sup>Medical School, Central Asian University, Tashkent 111221, Uzbekistan.

<sup>6</sup>Faculty of Chemistry, National University of Uzbekistan, Tashkent, 100034, Uzbekistan.

<sup>7</sup>Faculty of Chemistry, Semnan University, Semnan, Iran.

<sup>8</sup>Tashkent State University of Economics, Tashkent, 100066 Uzbekistan.

\*Corresponding Author.

Received 16/05/2023, Revised 10/07/2023, Accepted 12/07/2023, Published 05/12/2023



This work is licensed under a [Creative Commons Attribution 4.0 International License](https://creativecommons.org/licenses/by/4.0/).

### Abstract

In this research work, the novel polymer base on acrylamide N-methylene lactic and glycolic acid was synthesized and its structural performances were identified by the IR, 1H NMR and 13C NMR spectroscopic investigations. The influencing factors and kinetics of polymerization, viscosity performance were studied and quantum chemical calculations were used to identify the correlation between the structure and properties. It was determined that the polymerization rate of the examined monomers in an aqueous solution, in the presence of DAA, adheres to the standard rules for radical polymerization of acrylamide monomers in solution. An investigation into the pH solution's impact on the kinetics of radical polymerization of acrylamido-N-methylene glycolic and acrylamido-N-methylene lactic acids revealed an extreme dependence with a minimum in a neutral medium. It was found the linear correlation between pH and viscosity. The physical and chemical performance of this polymer depends on the structural parameters related the results of quantum chemical calculation. Biological tests conducted on polyacrylamido-N-methylene lactic acid indicated its potential as a plant growth stimulator. The polymeric form of lactic acid was found to enhance the growth of Dustlik variety wheat seedlings by 40% more efficiently than lactic acid alone.

**Keywords:** Glycolic acid, Lactic acid, pH-sensitive Hydrophilic Polymers, Polyacrylamide, Polymerization

### Introduction

Across the globe, interest in polymers is on the rise, particularly those whose properties are highly sensitive to subtle environmental changes. These polymers, known as stimulus-sensitive polymers, showcase a vast array of applications in fields, such

as medicine, pharmacy, biotechnology, ecology, and various other aspects of human life. They form the basis of stimulus-sensitive polymer gels<sup>1-3</sup>.

*Acrylamide.* Acrylamide ( $C_3H_5NO$ ) is a water-soluble, odorless, and colorless crystalline solid. It is widely used in the synthesis of polyacrylamide, a polymer with various applications ranging from water treatment, enhanced oil recovery, to the production of soft contact lenses and hydrogels.

*N-Methylene Lactic Acid.* N-Methylene lactic acid ( $C_4H_6O_3$ ) is an unsaturated hydroxyl acid derived from lactic acid. It is a versatile monomer used in the synthesis of biodegradable polymers, such as poly(N-methylene lactic acid).

*Glycolic Acid.* Glycolic acid ( $C_2H_4O_3$ ) is the smallest  $\alpha$ -hydroxy acid, known for its widespread use in skincare products. It is also a valuable monomer for the synthesis of biodegradable polymers, such as polyglycolic acid (PGA), which has applications in medical sutures, drug delivery systems, and tissue engineering.

Therefore, acrylamide, N-methylene lactic acid, and glycolic acid are essential monomers in the synthesis of various polymers through radical polymerization reactions. The polymerization process involves the use of initiators to generate free radicals, which react with monomers to propagate the polymer chain. By controlling reaction conditions, it is possible to tailor the properties of the resulting polymers for specific applications.

In recent years, the growing scope and application of synthetic polyelectrolytes, based on N-substituted amides with ionogenic groups, across various scientific, technological, biological, and medical fields have significantly heightened interest in the synthesis and formation mechanisms of these polymers. Radical polymerization and copolymerization of ionic monomers serve as a prevalent and accessible method for obtaining such polyelectrolytes. Investigating the characteristics of radical polymerization for new ionogenic monomers holds value from both fundamental and practical perspectives, as controlling the radical polymerization and copolymerization processes of these monomers enables the regulation of polymer composition, structure, and molecular weight<sup>4-7</sup>.

Globally, extensive research is conducted on the formation and physicochemical characteristics of stimulus-responsive polymers, focusing on several

key areas: exploring the kinetics and mechanisms involved in producing stimulus-responsive polymers; examining and controlling their pH and temperature-sensitive attributes; devising targeted delivery methods for medicinal compounds; and developing innovative technologies for isolating and purifying biologically active substances<sup>8-11</sup>.

For the first time, new monomers belonging to the N-substituted acrylamide series, derived from hydroxy acids with ionogenic functional groups, have been synthesized. The primary patterns of radical polymerization for acrylamido-N-methylene lactic and acrylamido-N-methylene glycolic acids were examined, resulting in pH-sensitive, water-soluble, and water-swelling polymers<sup>12-14</sup>.

It has been determined that the pH level of the medium and the ionic strength of the solution significantly influence the radical polymerization process of these monomers, thereby allowing for the regulation of this process. It was discovered that the acrylic monomer, in which the substituent is connected to the vinyl group by an ester bond, exhibits greater activity than the monomer that involves the amide bond for the addition. The reactivity difference between these monomers can be attributed to the varying mobility of the substituent at the double bond and the oxygen atom's higher electronegativity compared to the nitrogen atom. This results in a more pronounced reduction in electron density at the vinyl group of the monomer<sup>15-17</sup>.

The physicochemical properties of the produced polymers have been investigated, demonstrating the potential for controlling the stimulus-sensitive characteristics of copolymers based on their composition.

The study's objective is to synthesize novel polymers derived from natural hydroxy acids through the radical polymerization of their N-substituted acrylamides, explore the chemical transformation of polyacrylamide, and investigate certain physicochemical properties of the resulting polymers. Additionally, the research aims to identify promising applications for these polymers. Research methods employed include modern theoretical and experimental techniques, such as infrared (IR)

spectroscopy, nuclear magnetic resonance (NMR), viscometry, and elemental analysis.

## Materials

In this research work, the following chemicals (purchased from Bulgarian company) were used:

- i. Lactic acid - hygroscopic powder or syrup - liquid;  $T_{liq}=25-26^{\circ}\text{C}$ ;  $T_{boil}=103^{\circ}\text{C}$ ;  $d_4^{18}=1.2485\text{ g/cm}^3$ ; highly soluble in water, ethanol; slightly soluble in diethyl ether. A 40% aqueous solution of lactic acid was used.
- ii. Glycolic acid (HA) - colourless rhombic leaves;  $T_{liq}=79-80^{\circ}\text{C}$ ; soluble in water, ethanol.
- iii. Acrylamide (AA) -  $M=71.08$ ; colourless leaves;  $T_{liq}=84-85^{\circ}\text{C}$ ; soluble in water, ether.

## Methods

In this research work, the following methods were used:

- (i) IR spectroscopic analysis was done by using spectrometer Specord IR-75 in the area  $4000 - 400\text{ cm}^{-1}$ (KBr) (German company Analytik Jena).
- (ii)  $^1\text{H}$  NMR spectra were recorded on an NMR Unity 400 plus (Varian) ICPS ASRUz ( $\text{D}_2\text{O}$ ) spectrometer (United States).
- (iii)  $^{13}\text{C}$  NMR spectra were recorded with a BRUKER 600 MG spectrometer in ( $\text{D}_2\text{O}$ ) at the NMR spectroscopy laboratory of the University of Vienna (Austria).
- (iv) The polymer solutions' viscosity was measured using an Ubbelohde-type capillary viscometer, with a water flow time of 106.4 seconds. To determine the intrinsic viscosity, the Huggins equation was used to plot a system of dependencies, specifically the dependence of reduced viscosity on concentration. The reduced viscosity was calculated using the following ratios Eqs. 1, 2 and 3<sup>19,20</sup>:

$$\eta_{rel} = \tau/\tau_0 \quad 1$$

$$\eta_{sp} = \frac{\tau}{\tau_0} - 1 \quad 2$$

$$\eta_{pr} = \frac{\eta_{sp}}{c} \quad 3$$

- iv. Formalin -  $M= 30.03$ ; (40% aqueous paraform solution), colourless liquid with a sharp irritating odor;  $d_4^{18}=0.8153\text{ g/cm}^3$ .
- v. Azoisobutyric acid dinitrile (AAB) was recrystallized from a solution in ethanol before use. All the reagents and solvents used in the work were purified by known methods; the physicochemical parameters corresponded to the reference data.

Where  $\tau$  is the outflow time of the polymer solution,  $\tau_0$  is the outflow time of the pure solvent,  $C$  is the concentration of the polymer solution<sup>1-3</sup>.

- (v) The polymerization rate was calculated by Eq. 4:

$$V = Q \times [M]/3600 \times 100 \quad 4$$

Where,  $M$  is the monomer concentration, mol/l;  $Q$  is conversion, % hour;  $V$  is total polymerization rate, mol/l  $\times$  sec<sup>4-6</sup>.

In the field of polymer research, quantum chemical analysis proves to be a crucial tool due to the way in which a polymer molecule's structural properties impact its performance. This study employs various techniques to establish correlations between molecular structure and chemical properties. To conduct the quantum chemical analysis of selected compound, this research utilizes the GAMESS-US software with 6-21G basis sets, density functional theory (DFT), and B3LYP (which incorporates the three-parameter Lee-Yang-Parr correlation function by Becke). For purposes of visualization and analysis, wxMacMolPlt and Avogadro are utilized.

## Experimental Part

### Synthesis of Monomer

The synthesis of Acrylamide N-methylene lactic acid (AA-N-MLA) involved placing 7.1 g (0.1 mol) of acrylamide, 3 g (0.1 mol) of formalin, 9 g (0.1 mol) of lactic acid, and 0.03 g (0.002 mol) of

hydroquinone in a two-necked flask with a stirrer. Hydroquinone was added during the synthesis of Acrylamide N-methylene lactic acid to inhibit polymerization. Acrylamide was dissolved in a mixture containing formalin, lactic acid, and hydroquinone. Carbon tetrachloride and chloroform were used as solvents in the sequential extraction purification process of the synthesized product resulting in a yield of 70%. The mixture was stirred at 60°C for 3 hours, and the resulting product was subjected to water evaporation using a water jet pump at the same temperature. The target product was purified through sequential extraction via carbon tetrachloride and chloroform, resulting in a yield of 70%.

The synthesis of the methacryloylglycolic acid monomer (AA-N-MGA) was carried out in a 250 ml three-necked flask, which contained 15.2 g (0.2 mol) of glycolic acid, 100 ml of dioxane, and 44 ml (0.2 mol) of triethylamine. This mixture was cooled to 0°C, and with constant stirring, 18 ml (0.22 mol) of methacrylic acid chloride were added dropwise. After that, the temperature was raised to 333K and maintained for 2 hours. The mixture was then filtered, evaporated, and the residue about 50 ml

was vacuum distilled at a temperature of 371 K and a residual pressure of 10 mm. rt. Art. The resulting product was a transparent viscous liquid with a density of 1.0153 g/cm<sup>3</sup> at 420 nm and a refractive index of 1.4324 at 20°C. The yield of the product was 67%.

### Synthesis of Polymers

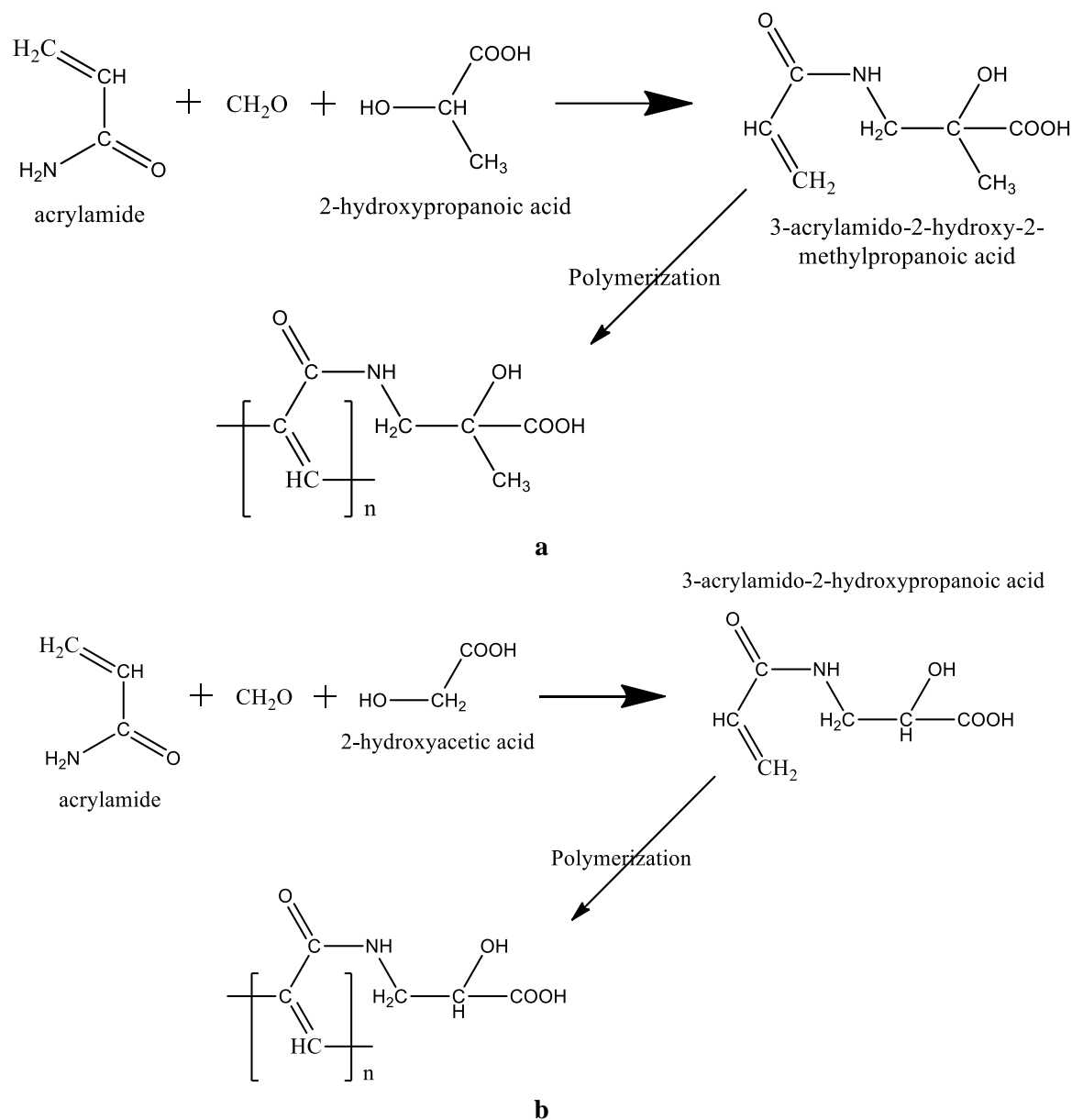
Polymerization of the resulting monomers was carried out in an aqueous solution in glass ampoules. After loading the ampoules with the required amount of initial reagents, the ampoules were degassed in vacuum to a residual pressure of 10<sup>-3</sup> mm Hg, sealed off and polymerized in a thermostat at a temperature of 60°C. The monomer concentration was 5% and the initiator concentration was 1% (Ratio is 5(Monomer):1(Initiator). Azoisobutyric acid dinitrile was used as the initiator. The resulting polymers were isolated by precipitation in isopropyl alcohol and dried under vacuum in a desiccator to constant weight<sup>7-9</sup>. The radical polymerization of the newly synthesized monomers: AA-N-MLA and AA-N-MGA were studied by the method of chemical initiation, using dinitrile of azoisobutyric acid (DAA) as an initiator in an aqueous solution by the dilatometric method, at 60°C<sup>10-12</sup>.

## Results and Discussion

### Molecular Interactions in Synthesis of Polymers

The choice of lactic acids as an object for obtaining a monomeric compound from them is due to the fact that the polymers of these compounds have polyelectrolyte properties, are non-toxic and non-immunogenic, and form CO<sub>2</sub> and H<sub>2</sub>O as a result of metabolic transformations in the body. Therefore, they are widely used in medicine for the manufacture of suture surgical threads and for obtaining

prolonged dosage forms. In the synthesis of acrylamido-N-methylene-lactic acid (AA-N-MLA) and acrylamide-N-methylene glycolic acid (AA-N-MGA), it was used the Mannich reaction. In this reaction, acrylamide interacts with formaldehyde, as a result of which methylolacrylamide is formed, then the latter interacts with a natural hydroxy acid, and as a result of the release of water, the corresponding N-substituted acrylamides of hydroxy acids are formed according to the following Scheme 1:



**Scheme 1. Synthesis of (a) acrylamido-N-methylene-lactic acid (AA-N-MLA) and (b) acrylamido-N-methylene glycolic acid (AA-N-MGA).**

### **IQ Analysis**

The chemical structure of the synthesized monomers was identified using IR spectra, molecular refraction (MR) calculations, and determination of the acid number by potentiometric titration. IR spectra of AA-N-MLA and AA-N-MGA are shown in Fig. 1 and Fig. 2. As can be seen from Fig. 1, in the IR spectrum of AA-N-MGA, the absorption bands are observed in the region of  $1620\text{ cm}^{-1}$ , corresponding

to the double bond and  $1680\text{ cm}^{-1}$  to the stretching vibrations of the  $-\text{CONH}-$  group of the monomer. An intense absorption band in the region of  $1345\text{ cm}^{-1}$  corresponds to  $-\text{OH}$  to the carboxyl group, and  $1720\text{ cm}^{-1}$  to the carbonyl of the carboxyl group of the hydroxy acid. At  $3353\text{ cm}^{-1}$ , an absorption band is observed corresponding to hydroxyl groups linked by hydrogen bonds, which indicates the dimerized state of the monomer<sup>7-9</sup>.



**Figure 1. IR spectrum of acrylamide-N-methylene glycolic acid (AA-N-MGA).**

The IR spectrum of AA-N-MLA Fig. 2 shows absorption bands in the region of  $1650\text{ cm}^{-1}$  is responsible for the double bond and  $1700\text{ cm}^{-1}$  shows the stretching vibrations of the  $-\text{CONH}-$  group of the monomer. An intense absorption band in the region of  $1445\text{ cm}^{-1}$  is attribute for the presence of  $-\text{OH}$  to the carboxyl group, and  $1680\text{ cm}^{-1}$  to the carbonyl of the carboxyl group of the hydroxy acid. At  $3753\text{ cm}^{-1}$ , an absorption band is observed indicates hydroxyl groups linked by hydrogen bonds, which indicates

the dimerized state of the monomer. It can be seen that the monomer is characterized by clear absorption bands in the region of  $3500\text{--}3000\text{ cm}^{-1}$ , which are characteristic of both OH stretching vibrations and amide groups, which makes accurate identification difficult. However, intense bending vibrations of the OH group was appeared around  $1100\text{ cm}^{-1}$  and stretching vibrations of the  $\text{C}=\text{O}$  bond of the carboxyl group was found in the region of  $1210\text{ cm}^{-1}$ , confirming the presence of carboxyl and hydroxyl<sup>10-12</sup>.

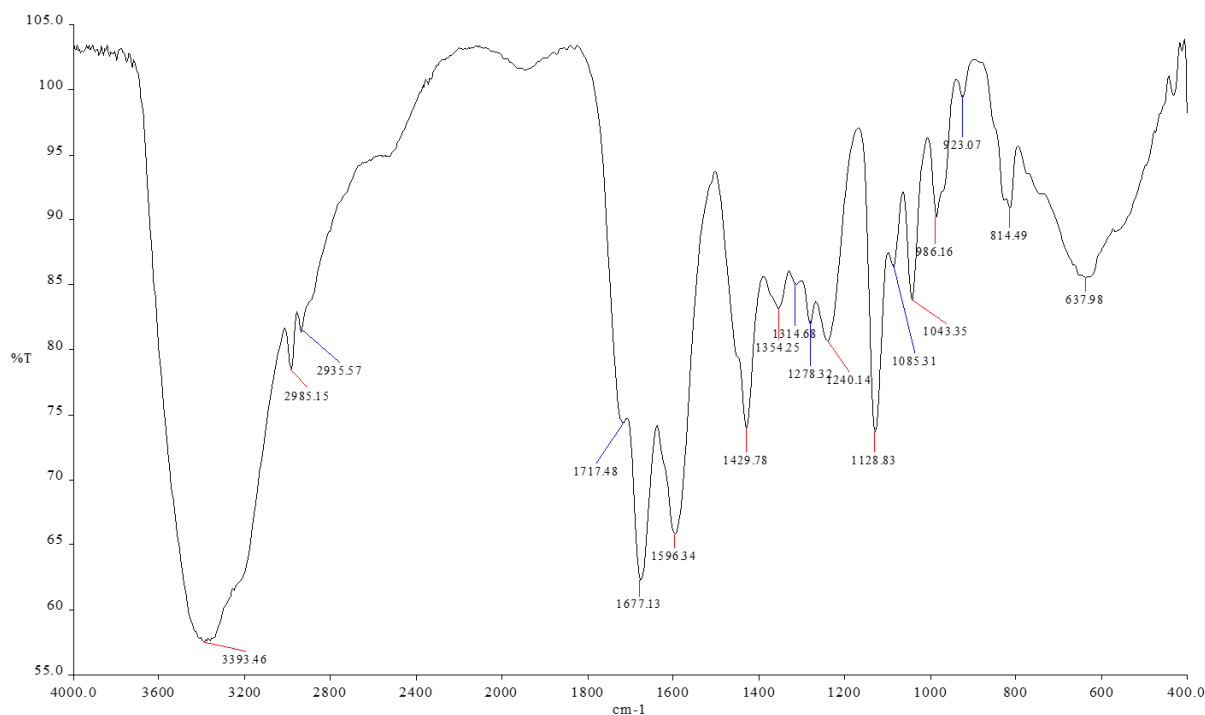


**Figure 2. IR spectrum of acrylamide-N-methylene-lactic acid (AA-N-MLA).**

### NMR Analysis

In the  $^1\text{H}$  NMR spectrum Fig. 3 at a frequency of 400 MHz for a solution of AA-N-MGA in heavy water, there are signal groups from an acrylic fragment at 6.18 ppm (2H) and 6.143 ppm (1H), as well as two equivalent doublets with 14 Hz splittings belonging to the protons of the  $\text{NCH}_2$  group centered at 3.39 ppm (equivalent to 1H) and 1.98 ppm (axial 1H). The signal at 4.88 ppm introduces the HD impurity into  $\text{D}_2\text{O}$  for the proton. The proton signals of hydroxyl groups and NH are not visible due to the exchange for deuterium in the  $\text{D}_2\text{O}$  medium. Thus, spectroscopic studies confirm the aforementioned formula of the synthesized compound.

In the PMR spectrum at 400 MHz of a solution of AA-N-MLA Fig.4 in heavy water, there are clusters of signals from an acrylic segment at 6.15 ppm (2H) and 5.703 ppm (1H), along with two corresponding doublets with 14 Hz splittings attributed to the protons of the  $\text{NCH}_2$  group centered at 4.09 ppm

(equivalent to 1H) and 1.947 ppm (axial 1H). The signal at 4.88 ppm brings the HD impurity into  $\text{D}_2\text{O}$  for the proton. The proton signals of hydroxyl groups and NH remain unseen due to the exchange for deuterium in the  $\text{D}_2\text{O}$  medium. Consequently, spectroscopic analyses verify the previously mentioned formula of the produced compound<sup>13-15</sup>.

In the  $^{13}\text{C}$  NMR spectra of the compounds Figs. 5 and 6, there are 20 ppm signals for the carbon atom of the methyl group, 60 ppm signals for carbon atoms of the hydroxyl group, 100-110 ppm signals for double bond carbon, and 180 ppm signals for carbon atoms of the carboxyl group. The presence of carboxyl groups in the monomers was also confirmed by potentiometric titration. Based on the literature data, NMR spectroscopy, and potentiometric titration, the reaction involving the interaction of acrylamide with hydroxy acids can be represented by the following scheme: where  $\text{R}=\text{H}$  is for a glycolic derivative, and  $\text{R}=\text{CH}_3$  is for a lactic acid derivative.

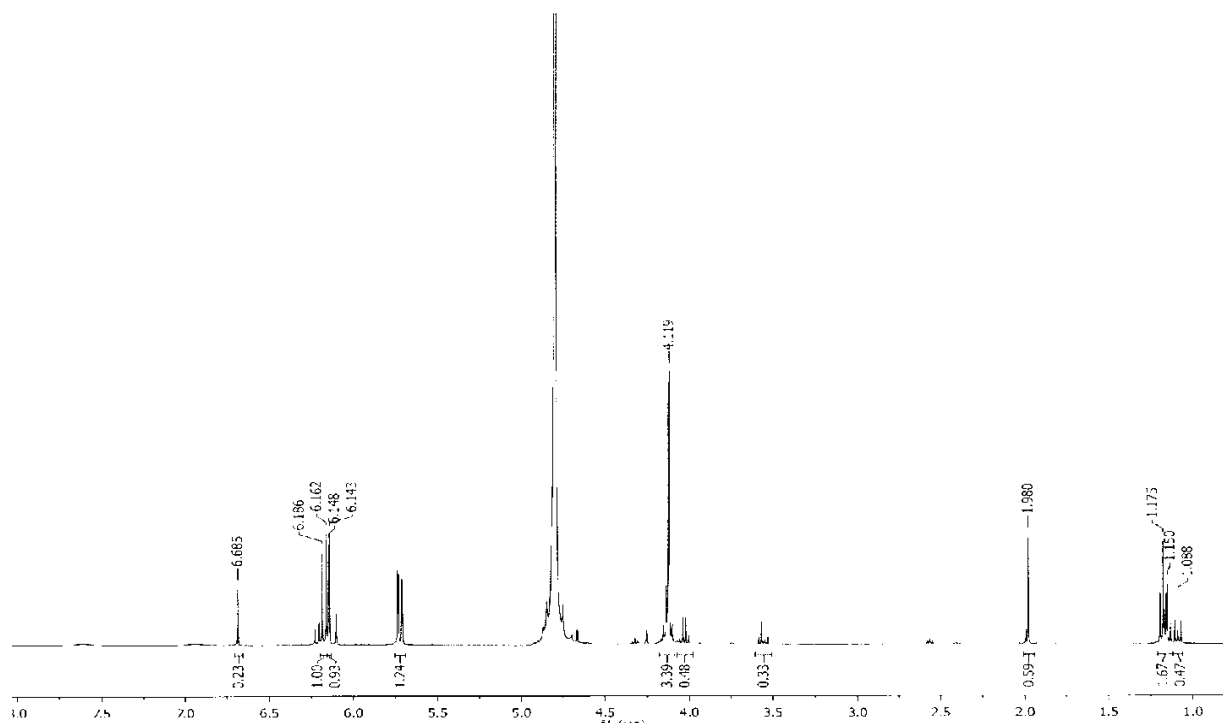


Figure 3.  $^1\text{H}$  NMR spectrum of acrylamide-N-methylene glycolic acid.

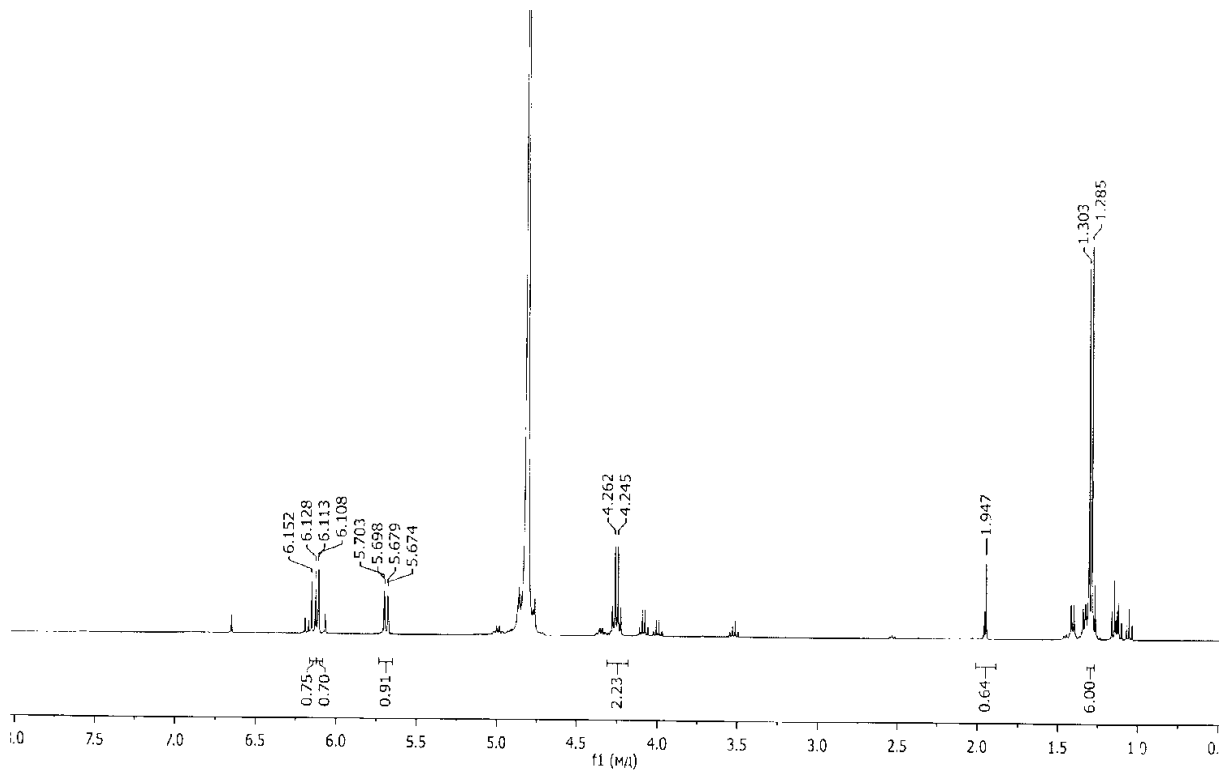


Figure 4. <sup>1</sup>H NMR spectrum of acrylamide-N-methylene-lactic acid.

Auftraggeber Lieberzeit  
L2

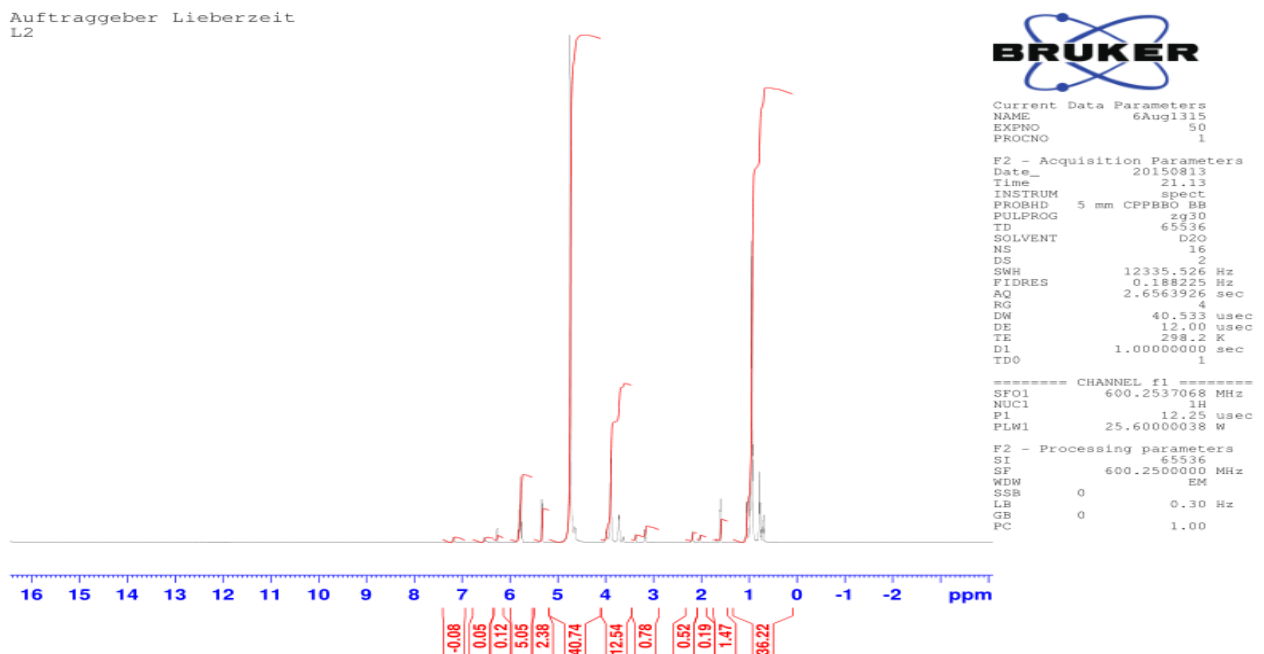


Figure 5. <sup>13</sup>C NMR spectrum of acrylamide-N-glycolic acid.



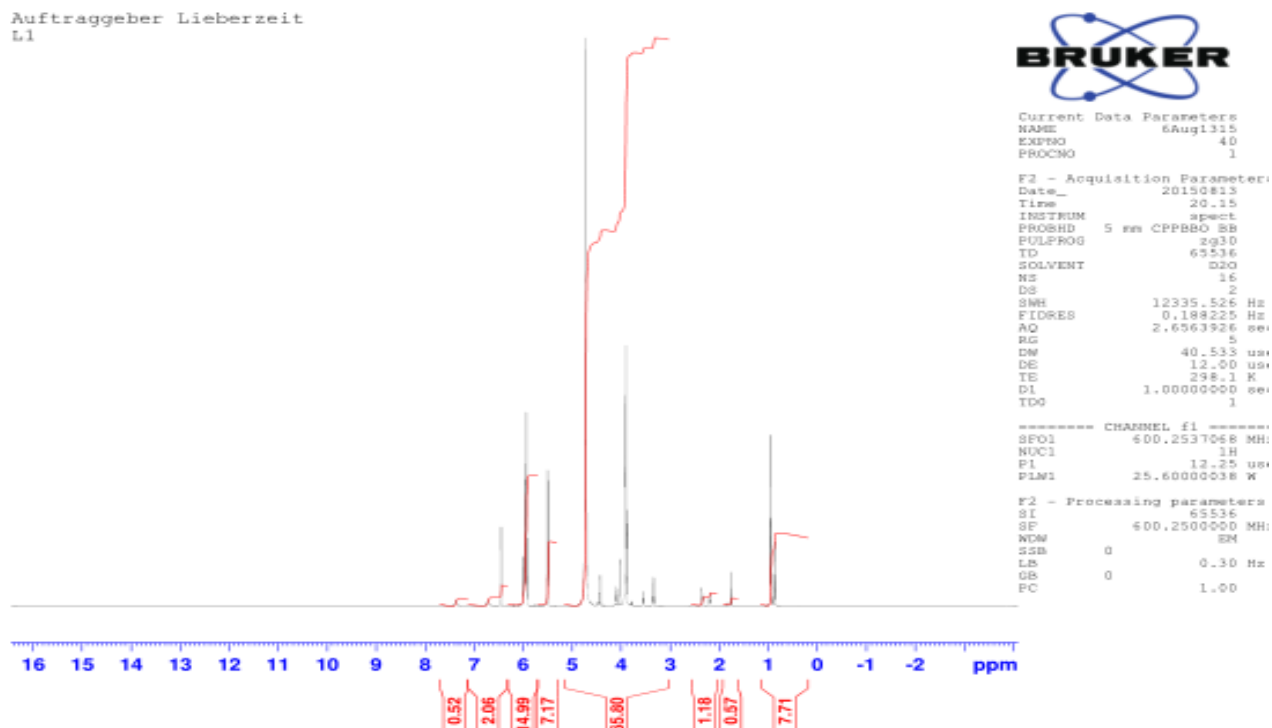


Figure 6.  $^{13}\text{C}$  NMR spectrum of acrylamide-N-lactic acid.

### Influence of Initiator's Concentration in the Rate of Polymerization

The radical polymerization of the newly synthesized monomers: AA-N-MLA and AA-N-MGA were studied by the method of chemical initiation, using dinitrile of azoisobutyric acid (DAA) as an initiator in an aqueous solution by the dilatometric method, at  $60^\circ\text{C}$ . In kinetic measurements, the conversion depth was within 10%. The contraction of monomers was calculated from the data on the polymer yield and volume reduction in the reaction system in homopolymerization and from the densities of polymer and monomer solutions, the value of which was AA-N-MLA-0.160 and AA-N-MGA-0.0676. Preliminary experiments showed that spontaneous polymerization of monomers does not occur under these conditions. When studying the polymerization kinetics, the concentration of the DAA initiator for AA-N-MLA varied from  $2.4 \times 10^{-3}$  to  $6 \times 10^{-3}$  mol/l, AA-N-MGA varied from  $0.73 \times 10^{-3}$  to  $2.9 \times 10^{-3}$  mol/l, and the monomer concentration is in the range of 0.15-0.6 mol/l. Figs. 7 and 8 show the kinetic curves of the polymerization of PAA-N-MLA and PAA-N-MGA obtained at different concentrations of the initiator DAA.

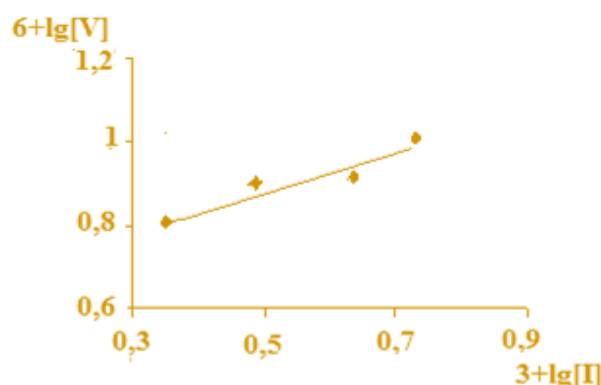
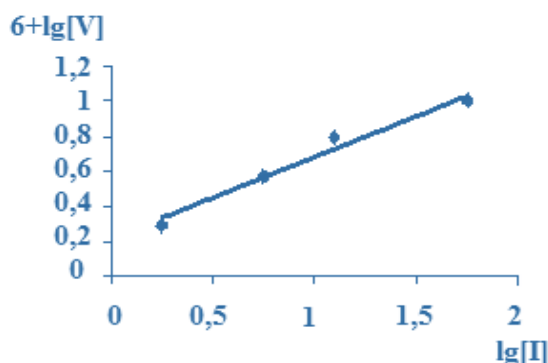


Figure 7. Dependence of PAA-N-MLA polymerization rate (V) on various initiator concentrations (I)  $[\text{M}]=0.6$  mol/l,  $\text{T}=333$ .

As observed from Figs. 7 and 8, the conversion of monomers into a polymer increases with both the concentration of the initiator and the duration of the polymerization reaction. Based on the logarithmic dependence of the polymerization rate on the initiator concentration Figs. 7 and 8, the reaction orders concerning the initiator were determined for each monomer. The obtained data indicate that for all studied monomers, the rate of polymerization in an aqueous solution is proportional to the initiator concentration raised to the power of  $0.5 \pm 0.05$ . This suggests that, under the examined conditions, the polymerization of monomers in an aqueous solution occurs under homogeneous conditions and is

accompanied by bimolecular termination of growing chains.



**Figure 8.** Dependence of PAA-N-MGA polymerization rate (V) on various initiator concentrations (I) [M]=0.6 mol/l, T=333.

#### Influence of Monomer's Concentration in the Pate of Polymerization

Figs. 9 and 10 present the results of investigating the kinetics of polymerization of PAA-N-MGA and PAA-N-MLA at various monomer concentrations. From the presented data, it is evident that the rate of polymerization of PAA-N-MGA and PAA-N-MLA in an aqueous solution increases with a rise in the concentration of monomers Figs. 9 and 10. Based on the data in Figs. 9 and 10, the orders of the polymerization reaction with respect to the monomer for PAA-N-MGA and PAA-N-MLA are determined as 1.89 and 1.37, respectively. The deviation in the order of the reaction in the monomer from the theoretical first, observed during the polymerization of PAA-N-MGA and PAA-N-MLA, suggests an association of these monomers, which is a characteristic feature of carboxylic acids.

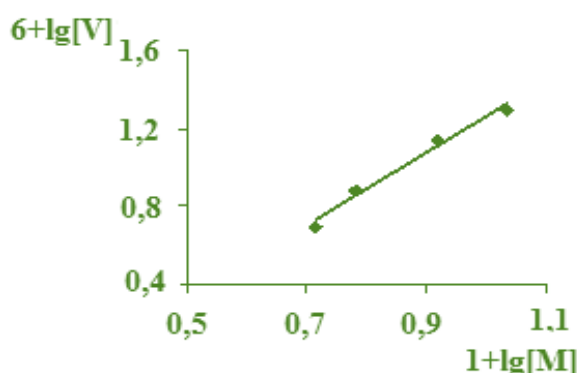


**Figure 9.** Dependence of PAA-N-MLA polymerization rate (V) on various monomer concentrations (M) [I]=  $6 \times 10^{-3}$  mol/l, T=333.

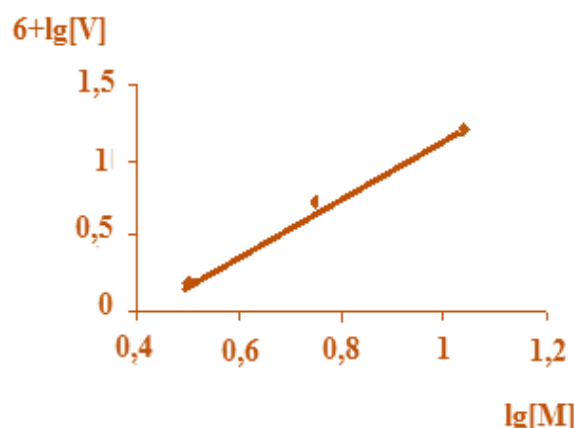


**Figure 10.** Dependence of PAA-N-MGA polymerization rate (V) on various monomer concentrations (M) [I]=  $1,76 \times 10^{-3}$  mol/l, T=333.

#### Kinetics of Polymerization

After studying the kinetics of radical polymerization of PAA-N-MGA and PAA-N-MLA in aqueous solutions at a temperature of 333K, it was derived the following general polymerization rate Eqs. 5 and 6:  
 For PAA-N-MGA  $V_n = K_m \times [I]^{0.5} \times [M]^{1.86}$  5  
 For PAA-N-MLA  $V_n = K_m \times [I]^{0.5} \times [M]^{1.37}$  6  
 The values obtained for m and n indicate that the polymerization of PAA-N-MGA and PAA-N-MLA in aqueous solutions, in the presence of DAA as an initiator, follows the typical patterns observed in the radical polymerization of acrylamides in solution. The difference in monomer order from the theoretical first order in the polymerization of monomers, as previously noted in the polymerization of acryloylglycolic acid, is explained by the characteristic association of these carboxylic acid monomers. Under the same conditions in radical polymerization, the activity of monomers can be arranged in the following order: PAA-N-MGA > PAA-N-MLA, which is likely due to an increase in the volume of substituents in the monomers.

To determine the temperature dependence and total activation energy of the polymerization of PAA-N-MGA and PAA-N-MLA, it was studied their polymerization at temperatures of 323, 333, and 343 K. An increase in temperature results in an increase in polymer yield for both PAA-N-MGA and PAA-N-MLA. The logarithmic dependences of the polymerization rate of PAA-N-MGA and PAA-N-MLA on reciprocal temperature are shown in Fig. 11. Based on these data, we calculated the values of the total activation energy of the process. The resulting values of  $E_a$  for PAA-N-MGA and PAA-N-MLA are

given in Table 1, respectively. It can be seen that these values correspond to the typical values

observed in the radical polymerization of vinyl monomers.

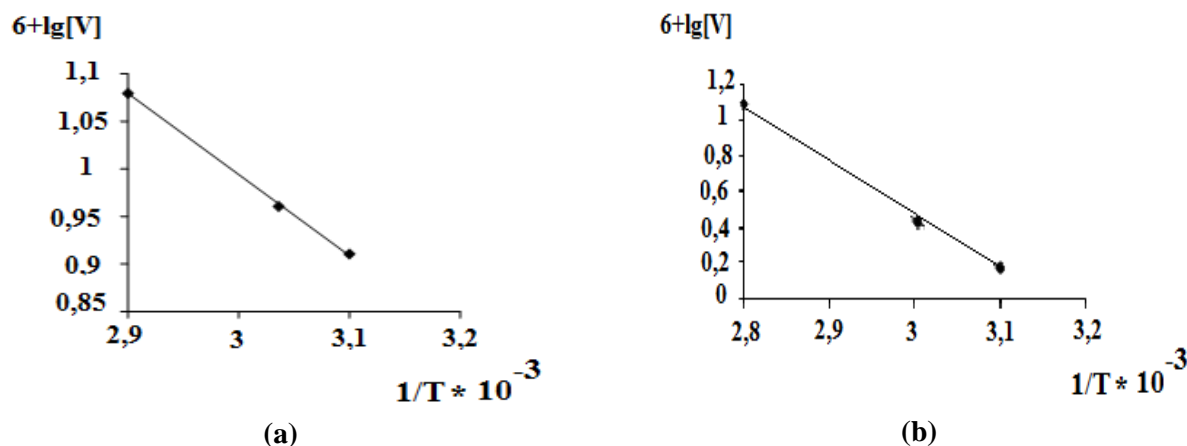


**Figure 11. Logarithmic dependence of the polymerization rate on temperature for (a) PAA-N-MLA and (b) PAA-N-MGA. (For PAA-N-MLA  $[M]=0.6$  mol/l,  $[I]=6\times 10^{-3}$  mol/l; for PAA-N-MGA  $[M]=0.3$  mol/l,  $[I]=2.9\times 10^{-3}$  mol/l.**

The results of studying the effect of temperature on the rate of polymerization of PAA-N-MLA and PAA-N-MGA made it possible to calculate the value of the total activation energy, which is about 70 kJ/mol (Table 1), which indicates a radical

mechanism of the polymerization reaction of PAA-N-MLA and PAA-N-MGA. The data obtained correspond to an increase in the polymerization rate, approximately 2-3 times, with an increase in temperature by 100 °C.

**Table 1. Kinetic parameters of radical polymerization of PAA-N-MLA ( $[M]=0.6$  mol/l,  $[I]=6\times 10^{-3}$  mol/l.) and PAA-N-MGA ( $[M]=0,3$  and mol/l,  $[I]=2.9\times 10^{-3}$  mol/l,) in aqueous solution.**

T, K	$V\times 10^{-6}$ mol/l×second		$E_a$ , kJ/mol	
	PAA-N-MLA	PAA-N-MGA	PAA-N-MLA	PAA-N-MGA
323	8.10	1.8		
333	9.05	7.1	67.0	75.2
343	11.90	8.5		

As is well-known<sup>5-8</sup>, ionizable monomers are highly sensitive to changes in the medium during radical polymerization and copolymerization in aqueous solutions. This is due to the fact that they exhibit additional factors such as dissociation, complexation, and electrostatic interactions, which have a significant influence on their reactivity in radical addition reactions, the kinetics of the process, and the mechanism of its elementary stages<sup>9,10</sup>. Since PAA-N-MLA and PAA-N-MGA contain ionic functional groups, it becomes necessary to study the effect of various factors on the polymerization reaction rate, such as the presence of low molecular weight salts and the pH value of the medium, which can alter the dissociation ability of ionogenic groups. Previous studies have shown a similar dependence of the effect of pH on the polymerization rate, and it

was of interest to investigate whether a similar pattern persists for acrylamide derivatives containing acidic groups. Therefore, we studied the kinetics of radical polymerization of these monomers in aqueous solutions at various pH values and ionic strengths using the dilatometric method. The pH values of the solution medium were adjusted by adding appropriate amounts of HCl and NaOH. The results obtained showed an extreme dependence of the logarithmic polymerization rate on the pH of the medium, with a minimum observed at neutral pH, Figs. 12 and 13.

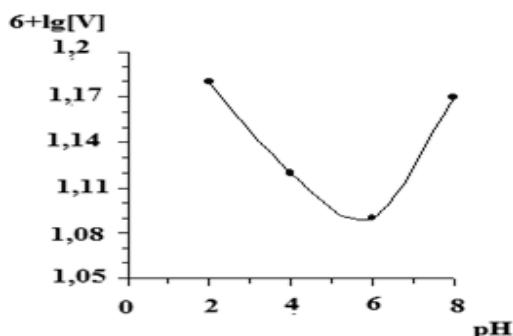


**Figure 12.** Dependence of the yield of PAA-N-MLA polymerization rate on the pH of the solution medium ( $[M]= 0.6 \text{ mol/l}$ ,  $[I]= 6 \times 10^{-3} \text{ mol/l}$ ,  $T=333 \text{ K}$ ).

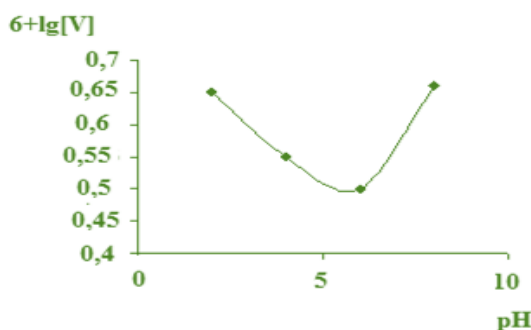


**Figure 13.** Dependence of the yield of PAA-N-MGA polymerization rate on the pH of the solution medium ( $[M]= 0.29 \text{ mol/l}$ ,  $[I]= 2.9 \times 10^{-3} \text{ mol/l}$ ,  $T=333 \text{ K}$ ).

To obtain new reactive polymers with stimulus-sensitive properties, we studied the kinetics of radical polymerization of acrylamido-N-methylene-lactic and glycolic acids. The usual patterns observed for vinyl monomers were observed in their radical polymerization, and the reactivity of the monomers increased in the series PAA-N-MGA>PAA-N-MLA, depending on the nature of the bond between the vinyl group and the substituent. The presence of

ionogenic groups in the monomers had a significant effect on their reactivity, with the rate of radical polymerization being higher in acidic and alkaline media than in neutral. Addition of a neutral salt to their aqueous solution also led to an increase in the rate of polymerization. The observed effects were due to an increase in the value of  $K_p/K_o$  is 0.5, indicating a change in the reactivity of the monomers in the corresponding media and submission of the process of polymerization to the theory of ion pairs of Kabanov and Topchiev.

### Viscosity of Polymer Solutions

PAA-N-MGA and PAA-N-MLA are white powders that are soluble in water, methanol, ethanol, DMF, DMSO, and some other polar solvents, but insoluble in ethers, benzene, and hydrocarbons. The physicochemical properties of polyelectrolyte solutions differ from those of nonelectrolyte polymers, with the presence of ionizable groups having a strong effect on viscosity. Ionization of the macromolecule leads to repulsive forces between like-charged groups, resulting in a significant change in the conformation of macromolecules in solution and deviation from the rectilinear dependence  $\eta_{sp}/C=f(C)$ . The reduced viscosity of aqueous solutions of PAA-N-MLA and PAA-N-MGA as a function of polymer concentration is shown in Fig.14. Diluting aqueous solutions of PAA-N-MLA and PAA-N-MGA leads to a significant increase in reduced viscosity, which is characteristic of polyelectrolytes and explained by the effect of "polyelectrolyte swelling." As polyelectrolytes, ionization of the carboxyl groups of PAA-N-MLA and PAA-N-MGA increases when their aqueous solutions are diluted, leading to swelling of the polymer chains.

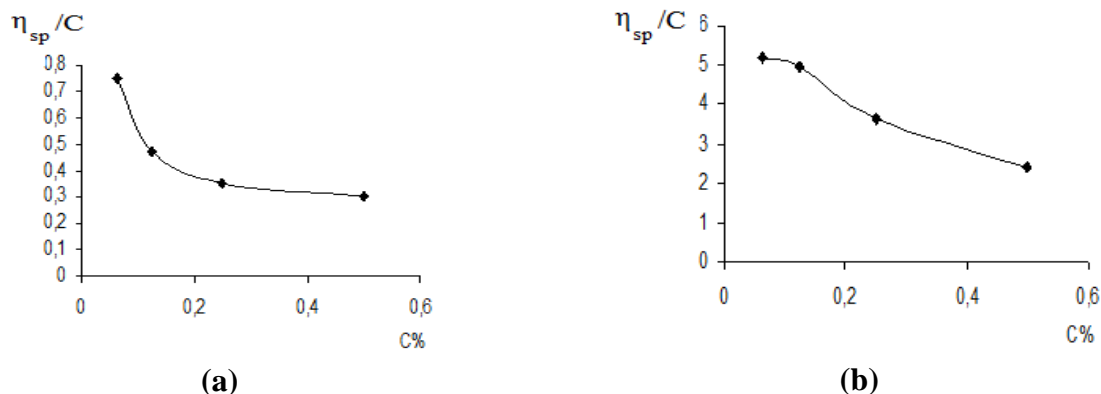


**Figure 14.** Dependence of the reduced viscosity of aqueous solutions of (a) PAA-N-MLA and (b) PAA-N-MGA on the polymer concentration.

The Fuoss Eq.6 was used to process the data of viscometric measurements of aqueous solutions of PAA-N-MLA and PAA-N-MGA.

$$\frac{C}{\eta_{sp}} = \frac{1}{A} + \frac{B}{A}\sqrt{C} \quad (6)$$

The reduced viscosity of polymer solutions is typically linear with concentration, as shown in Fig. 14, but this is not the case for polyelectrolytes due to the presence of ionizable groups. These groups create repulsive forces between like-charged units, causing a change in macromolecule conformation and deviation from the linear relationship  $\eta_{sp}/C=f(C)$ . The effect of polyelectrolyte swelling leads to a significant increase in viscosity upon dilution, as seen in the increased reduced viscosity of PAA-N-MLA and PAA-N-MGA solutions in Fig.14. This swelling is caused by additional dissociation of carboxyl groups and electrostatic repulsion of charged chain units, resulting in increased macromolecule charge and swelling. However, polyelectrolyte swelling can be mitigated by introducing a neutral low molecular weight electrolyte or maintaining a constant ionic strength of the solution, as shown in Fig. 15.

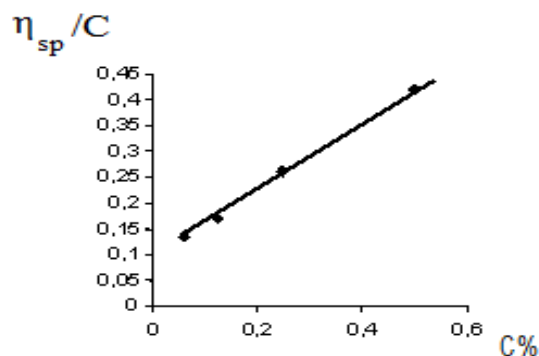
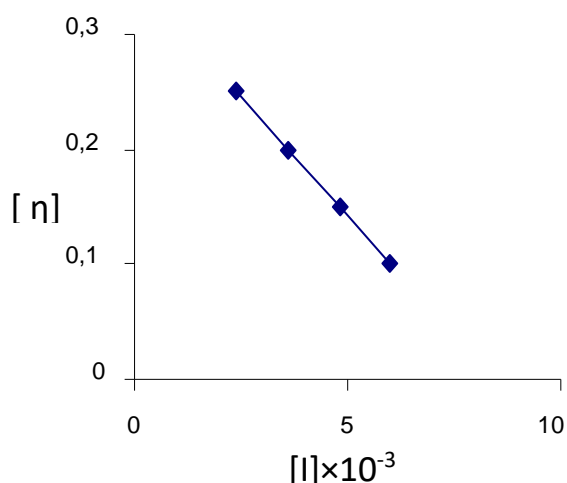
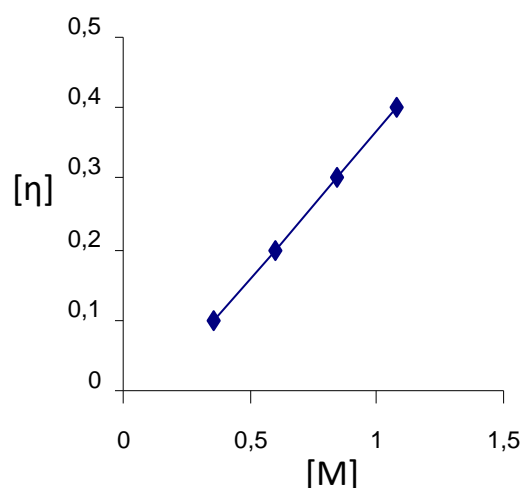


**Figure 15.** The dependence of the reduced viscosity of poly AA-N-MLA in a 0.5 N solution of KCl.

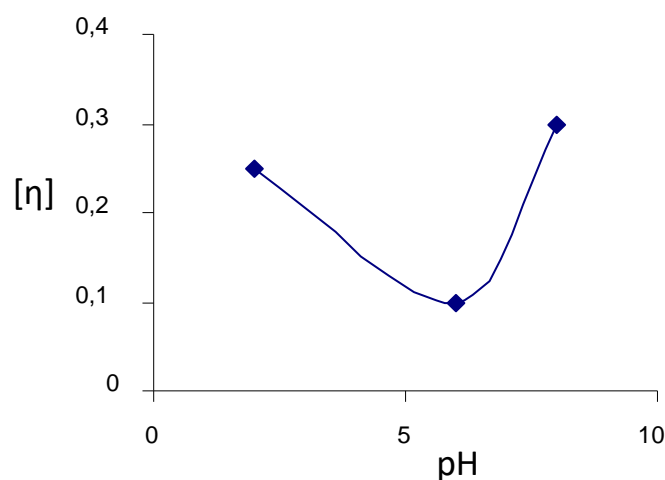
Fig.16 depicts the relationship between the intrinsic viscosity of PAA-N-MLA and the concentration of the initiator, monomer, and pH medium. Similar viscosity measurements were obtained for PAA-N-MGA. The figures demonstrate that the intrinsic viscosity of the polymers decreases as the initiator concentration increases, but increases with an increase in monomer concentration. Additionally, the intrinsic viscosity is symbiotic with the change in polymerization rate at different pH values of the medium. This symbiotic relationship provides further evidence for the proposed mechanism of radical polymerization of the studied monomers in aqueous solutions.



(a)



(b)



(c)

**Figure 16. Dependence of the intrinsic viscosity of PAA-N-MLA on the concentration of the initiator, monomer, and pH medium.**

### Quantum Chemical Analysis

In acrylamides, it was discovered that glycolic acid is connected by a rigid amide bond, whereas in AA-N-MGA and AA-N-MLA, the substituent is linked through a more flexible, rotating ester bond. Consequently, the steric hindrance in the polymerization of AA-N-MLA is significantly lower than that of AA-N-MGA, resulting in a higher activity of the ester monomer. Furthermore, the electron density of the double bond in the ester monomer shifts more towards the substituent due to its increased electronegativity, facilitating double bond cleavage and enhancing reactivity<sup>20,21</sup>. Quantum mechanical calculations corroborate our findings regarding the superior reactivity of AA-N-MLA in comparison to acrylamide monomers, as the ester group withdraws electron density from the double bond more effectively than the amide group<sup>22-25</sup>.

The proportional locations of functional groups, heteroatoms, and basic chains of examined monomers reveal the planar characteristic of the chosen system. Figures 17a and 18a demonstrate that the selected monomers form a more planar molecular structure. This examination presents increased negative and positive charged areas within the optimized configuration. The charge values were dispersed throughout the entire molecule because the  $\pi$ -electron systems, heteroatoms, and highly active functional groups primarily contribute to the charge distribution<sup>26,27</sup>. Furthermore, the polar architecture affects the charge dispersion. It was discovered that the nitrogen atoms within amino functional groups possess a higher negative charge<sup>28-30</sup>.

The optimal electrophilic and nucleophilic centers are determined through molecular electrostatic potential (MEP) evaluation. Figs. 17b and 18b depict the MEP of AA-N-MGA and AA-N-MLA, verifying that the chosen molecule is a more nucleophilic compound. The red and blue areas within this MEP indicate electrophilic and nucleophilic centers. Nucleophilic regions are accountable for chemical interactions, whereas electrophilic regions facilitate re-chemical interactions.

The electron allocation in HOMO and LUMO areas was determined by the frontier molecular orbital (FMO) examination. The HOMO and LUMO areas primarily contribute to the electron transfer's donation and acceptance performance, meaning that the electrons of the substrate in HOMO areas AA-N-MGA and AA-N-MLA, Figs. 17c and 18c are conveyed to reactant vacant orbitals (Fe), while some electrons in occupied orbitals of the reactant are re-conveyed to the substrate LUMO areas (AA-N-MGA and AA-N-MLA, Figs. 17d and 18d). Coordination bonds are established during electron transfer processes.

Various chemical parameters serve as valuable indicators in describing chemical performance. These parameters are calculated in relation to Eqs. 7-14, with the results displayed in Table. 2. The energies of HOMO ( $E_{HOMO}^{DFT}$ ) and LUMO ( $E_{LUMO}^{DFT}$ ) are utilized to compute different reactivity parameters. The following conclusions were drawn from the data observed in Table 2. The values in dipole moment, electron affinity ( $A^{DFT}$ ), molecular ionization potential ( $I^{DFT}$ ), electronic negativity

( $\chi^{DFT}$ ), global electrophilicity index ( $\omega^{DFT}$ ), electronic chemical potential ( $\mu^{DFT}$ ), and nucleophilicity ( $\epsilon^{DFT}$ ) enhance the high reactivity of the optimized AA-N-MGA and AA-N-MLA molecules. The DFT outcomes corroborate the experimental research. The energy difference ( $\Delta E^{DFT}$ ) between the HOMO and LUMO energies for the optimized AA-N-MGA and AA-N-MLA molecules illustrates the chemical reactivity of the structure. It was determined that the value in was low, signifying that the chosen compound is more reactive<sup>30-33</sup>. The values in chemical softness ( $\sigma^{DFT}$ ) for this inhibitor are considerably higher than those in chemical hardness ( $\eta^{DFT}$ ), indicating that the selected compound is a softer molecule. Good

chemically soft molecules possess low charge states and exhibit strong polarizability<sup>34-37</sup>.

$$\Delta E^{DFT} = E_{LUMO}^{DFT} - E_{HOMO}^{DFT} \quad 7$$

$$I^{DFT} = -E_{HOMO}^{DFT} \quad 8$$

$$A^{DFT} = -E_{LUMO}^{DFT} \quad 9$$

$$\eta^{DFT} = \frac{1}{2}(I^{DFT} - A^{DFT}) \quad 10$$

$$\epsilon^{DFT} = \frac{1}{\omega^{DFT}} \quad 11$$

$$-\mu^{DFT} = \chi^{DFT} = \frac{1}{2}(I^{DFT} + A^{DFT}) \quad 12$$

$$\omega^{DFT} = \frac{(\chi^{DFT})^2}{2\eta^{DFT}} \quad 13$$

$$\sigma^{DFT} = \frac{1}{\eta} \quad 14$$

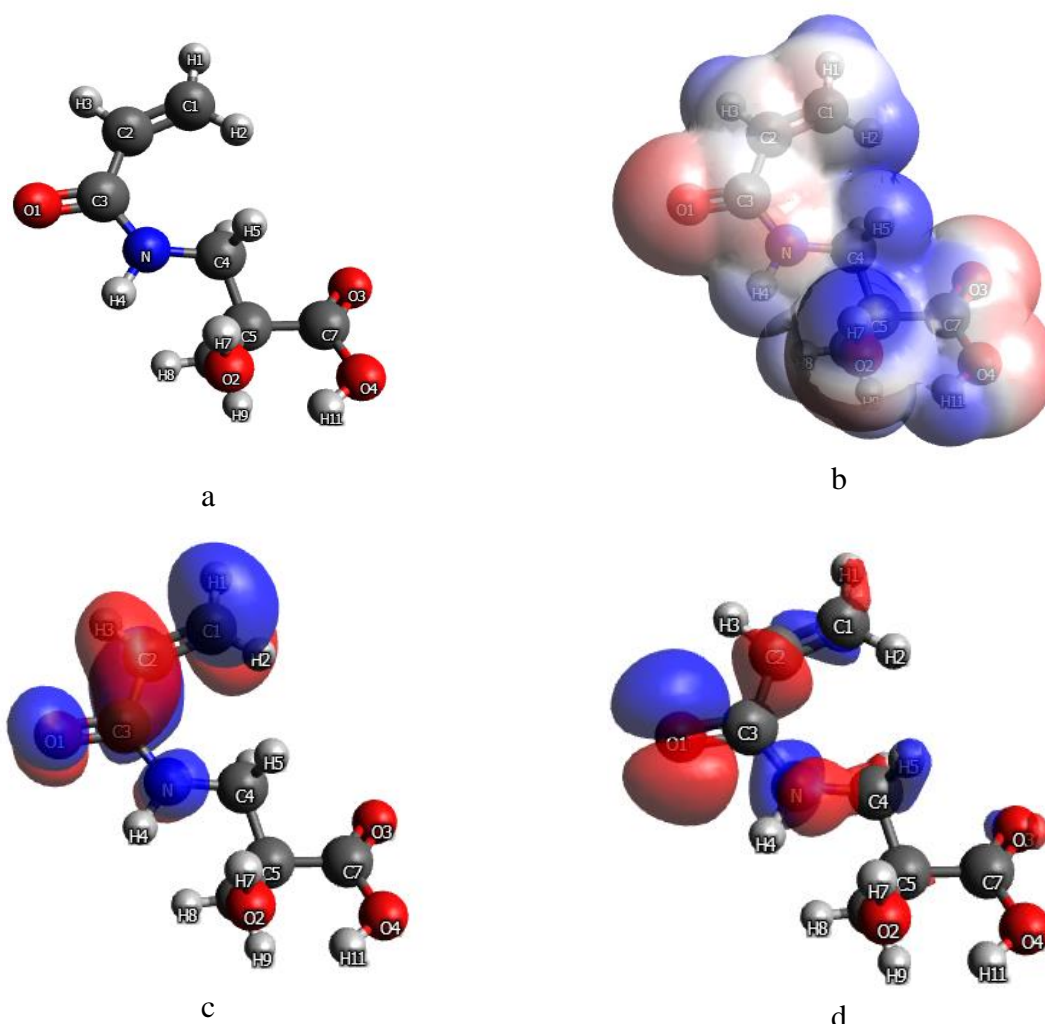


Figure 17. (a) Optimised structure, (b) MEP, (c) LUMO and (d) HOMO of AA-N-MLA.

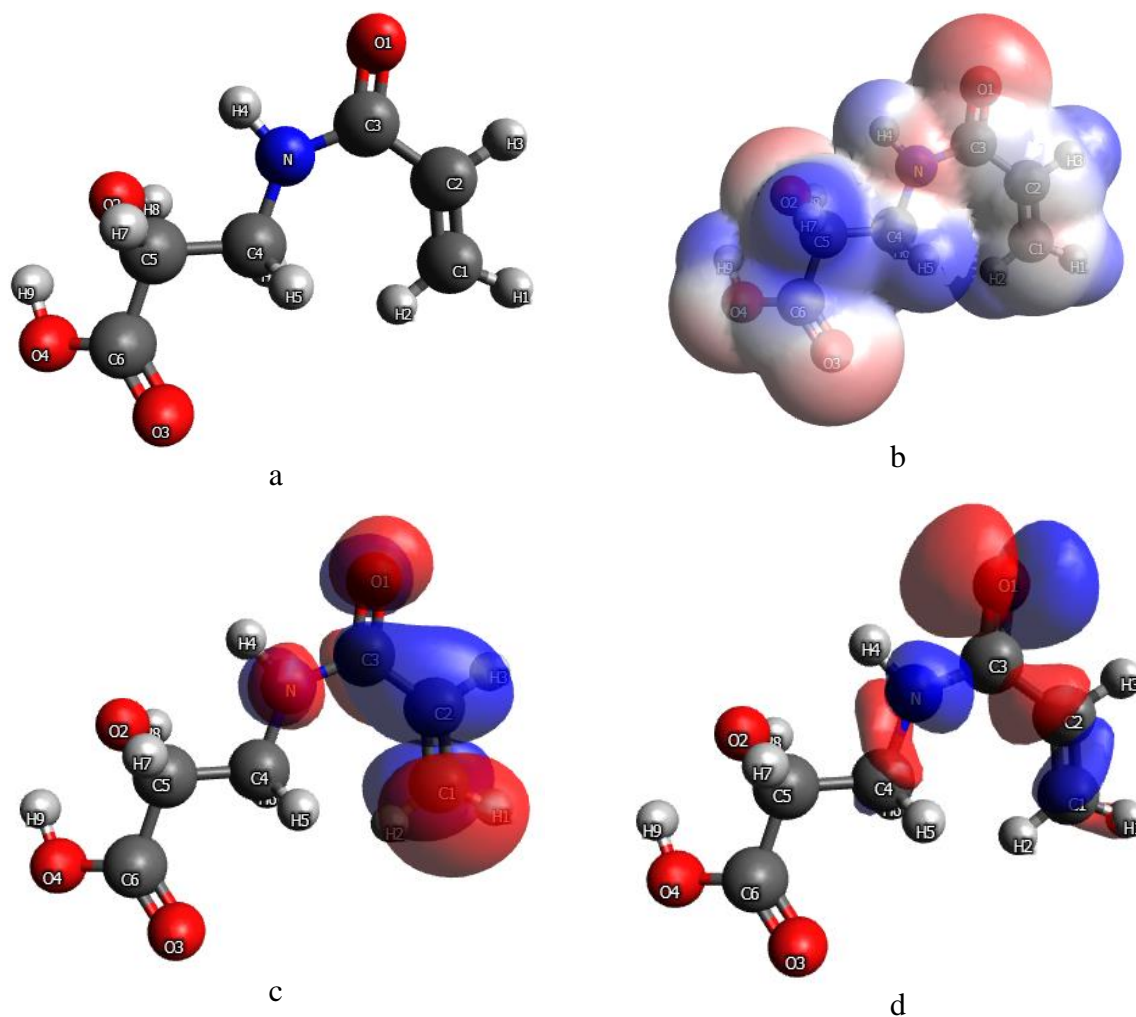


Figure 18. (a) Optimised structure, (b) MEP, (c) LUMO and (d) HOMO of AA-N-MGA.

Table 2. Theoretical parameters for AA-N-MGA and AA-N-MLA (DFT, B3LYP and 6-31G(d) basis sets).

Parameter	Values (eV)	
	AA-N-MLA	AA-N-MGA
$E_{HOMO}^{DFT}$	-178.071	-177.479
$E_{LUMO}^{DFT}$	-25.471	-24.801
$\Delta E^{DFT}$	152.6	152.7
$\sigma^{DFT}$	0.013	0.0131
$\omega^{DFT}$	395.13	390.25
$\eta^{DFT}$	76.3	76.34
$\chi^{DFT}$	101.771	101.14
$I^{DFT}$	178.071	177.479
$A^{DFT}$	25.471	24.801
$\mu^{DFT}$	-101.771	-101.14
$\epsilon^{DFT}$	0.0025	0.00256
Dipole moment, D	2.392	2.437



### Applications of Produced Polymer

Impact of AA-N-MLA on seed sprouting and vegetative development of wheat saplings. Plant growth enhancers are increasingly gaining prominence. They aid in boosting the yield of diverse crops and enhancing the quality of agricultural produce. The economic advantage from employing synthetic growth enhancers significantly surpasses the expense of obtaining them. Many of these enhancers have been practically applied. However, their widespread distribution faces obstacles, primarily due to the current situation where a drastic decline in the production of numerous synthetic substances, including plant growth enhancers, results in scarcity, subsequently raising their prices. Secondly, like all biologically active compounds, growth enhancers necessitate cautious handling. Overdosing such compounds may not only fail to yield the anticipated effect but also lead to contrasting outcomes. In this context, the concentration scope of growth enhancers is typically narrow and distinct for various plant development stages, making the likelihood of overdose quite high.

Most importantly, the mechanism through which enhancers impact plant growth processes remains largely unclear, rendering it impossible to foresee the effect on a living being (human or animal) of agricultural goods cultivated using growth enhancers. Table .3 demonstrates the impact of assorted carboxylic acids, encompassing hydroxy acids, on radish yield.

The impact of lactic acid polymer on wheat productivity was investigated at the Tokhtaev Komil Tokhtaevich farm, located in the Shahrizabz district of the Kashkadarya region. The results obtained are displayed in the table below. As evident from the table, both lactic acid and its polymeric form significantly influence seed germination and the vegetative growth of wheat seedlings. For instance, the germination rate of the "Sayhun" wheat variety increases from 10% to 15%, while the "Dostlik" variety experiences an increase from 8% to 14%. The table also highlights that as the concentration of the polymer solution rises, the germination yield correspondingly increases.

**Table 3. Examining the impact of PAA-N-MLA on seed germination and vegetative growth of wheat seedlings named *Saihun* (S) and *Dostlik* (D).**

Concentration	Wheat type	Germination, %	Productivity	
			Control	Under stimulator of selected polymer
1×10 <sup>-7</sup> M	S	10	22	24
	D	8	23	25
1×10 <sup>-6</sup> M	S	12	22	25
	D	11	23	26
1×10 <sup>-5</sup> M	S	15	22	26
	D	14	23	27

### Conclusion

The study's objective is to synthesize novel polymers (acrylamide with methylene lactic and glycolic acid) derived from natural hydroxy acids through the radical polymerization of their N-substituted acrylamides, explore the chemical transformation of polyacrylamide, and investigate certain physicochemical properties of the resulting polymers. Additionally, the research aims to identify promising applications for these polymers. As a results, the following conclusions were found:

(i) To synthesize pH-sensitive hydrophilic polymers, acrylamido-N-methylene glycolic and acrylamido-N-methylene lactic acids were

created for the first time using natural hydroxy acids as a foundation. The structures of these synthesized monomers were identified through IR spectroscopy and various physicochemical analytical methods.

(ii) The kinetics of radical polymerization for acrylamido-N-methylene glycolic and acrylamido-N-methylene lactic acids in aqueous solutions were studied. It was determined that the polymerization rate of the examined monomers in an aqueous solution, in the presence of DAA, adheres to the standard rules for radical polymerization of acrylamide

monomers in solution. The differing reactivity of these monomers is attributed to the distinct mobility of the substituent at the double bond and the oxygen atom's higher electronegativity compared to the nitrogen atom, resulting in a more significant reduction in electron density at the vinyl group of the monomer.

- (iii) An investigation into the pH solution's impact on the kinetics of radical polymerization of acrylamido-N-methylene glycolic and acrylamido-N-methylene lactic acids revealed an extreme dependence with a minimum in a neutral medium.
- (iv) By examining the effects of pH and temperature on the viscosity of aqueous solutions, as well as the swelling and collapse kinetics of cross-linked polymers and copolymers based on

natural hydroxy acids and their compositions, it was determined that they exhibit pH- and thermosensitive properties. The presence of both amide and carboxyl groups in the polymer composition results in a unique feature: two critical mixing temperatures within a narrow temperature range.

- (v) Biological tests conducted on polyacrylamido-N-methylene lactic acid indicated its potential as a plant growth stimulator. The polymeric form of lactic acid was found to enhance the growth of Dustlik variety wheat seedlings by 40% more efficiently than lactic acid alone.
- (vi) A water-soluble polymer based on lactic acid was introduced as a plant growth stimulator at a farm in the Shakhriyab district of the Kashkadarya region.

## Acknowledgment

Authors thanks to Faculty of Pharmacy, Tashkent Pharmaceutical Institute, Tashkent, Uzbekistan, for support.

## Authors' Declaration

- Conflicts of Interest: None.
- We hereby confirm that all the Figures and Tables in the manuscript are ours. Furthermore, any Figures and images, that are not ours, have been

included with the necessary permission for re-publication, which is attached to the manuscript.

- Ethical Clearance: The project was approved by the local ethical committee in Tashkent Pharmaceutical Institute.

## Authors' Contribution Statement

S. K. Conception, design, drafting the MS.  
N. Z. Drafting the MS.  
B. M. Analysis.  
B. L. Interpretation.  
O. K. Acquisition of data.

G. A. Interpretation.  
E. B. Conception, design, drafting the MS, revision and proofreading.  
A. H. B. Revision and Proofreading.  
A.N. Revision

## References

1. Biswas A, Shukla A, Maiti P. Biomaterials for interfacing cell imaging and drug delivery: An overview. *Langmuir*. 2019; 35 (38):12285-12305. <https://doi.org/10.1021/acs.langmuir.9b00419>
2. Retnaningtyas Y, Supriyanto G, Irawan R, Siswodihardjo S. Noncovalently D-arabinitol Molecularly Imprinted Polymers (MIPs) to Identify Different Sugar Alcohols. *Baghdad Sci J*. 2021; 30 (18): 1536. [https://doi.org/10.21123/bsj.2021.18.4\(Suppl.\).1536](https://doi.org/10.21123/bsj.2021.18.4(Suppl.).1536)
3. Zhang A, Jung K, Li A, Liu J, Boyer C. Recent advances in stimuli-responsive polymer systems for remotely controlled drug release. *Prog Polym Sci*. 2019; 99: 101164. <https://doi.org/10.1016/j.progpolymsci.2019.101164>
4. Al-Issa MA, Mohammed AH. Copolymerization of Acrylamide with Acrylic acid. *Baghdad Sci J*. 2012; 9(2): 285-8. <https://doi.org/10.21123/bsj.2012.9.2.285-288>
5. Rizwan M, Gilani SR, Durani AI, Naseem S. Materials diversity of hydrogel: Synthesis, polymerization process and soil conditioning properties in agricultural field. *J Adv Res*. 2021; 33: 15-40. <https://doi.org/10.1016/j.jare.2021.03.007>

6. Andrade F, Roca-Melendres MM, Durán-Lara EF, Rafael D, Schwartz Jr S. Stimuli-responsive hydrogels for cancer treatment: The role of pH, light, ionic strength and magnetic field. *Cancers*. 2021; 13(5): 1164. <https://doi.org/10.3390/cancers13051164>
7. Babaluei M, Mottaghitlab F, Seifalian A, Farokhi M. Injectable multifunctional hydrogel based on carboxymethylcellulose/polyacrylamide/polydopamine containing vitamin C and curcumin promoted full-thickness burn regeneration. *Int J Biol Macromol*. 2023; 236: 124005. <https://doi.org/10.1016/j.ijbiomac.2023.124005>
8. Daliri K, Pfannkuche K, Garipcan B. Effects of physicochemical properties of polyacrylamide (PAA) and (polydimethylsiloxane) PDMS on cardiac cell behavior. *Soft Matter*. 2021; 17(5): 1156-1172. <https://doi.org/10.1039/D0SM01986K>
9. Sung YK, Kim SW. Recent advances in polymeric drug delivery systems. *Biomater Res*. 2020 Dec; 24(1): 1-2. <https://doi.org/10.1186/s40824-020-00190-7>
10. Arican F, Uzuner-Demir A, Sancakli A, Ismar E. Synthesis and characterization of superabsorbent hydrogels from waste bovine hair via keratin hydrolysate graft with acrylic acid (AA) and acrylamide (AAm). *Chem Pap*. 2021; 75: 6601-6610. <https://doi.org/10.1007/s11696-021-01828-z>
11. Mi HY, Jiang Y, Jing X, Enriquez E, Li H, Li Q, Turng LS. Fabrication of triple-layered vascular grafts composed of silk fibers, polyacrylamide hydrogel, and polyurethane nanofibers with biomimetic mechanical properties. *Mater Sci Eng C*. 2019; 98: 241-9. <https://doi.org/10.1016/j.msec.2018.12.126>
12. Yang J. PLGA microsphere/P (NIPAAm-co-AAm) hydrogel combination systems for drug delivery. *IOP Conf Ser.: Mater Sci Eng*. 2019; 504(1): 012013. <https://doi.org/10.1088/1757-899X/504/1/012013>
13. Gorantla S, Waghule T, Rapalli VK, Singh PP, Dubey SK, Saha RN, Singhvi G. Advanced hydrogels based drug delivery systems for ophthalmic delivery. *Recent Pat Drug Deliv Formul*. 2019; 13(4): 291-300. <https://doi.org/10.2174/1872211314666200108094851>
14. Zou F, Xu J, Yuan L, Zhang Q, Jiang L. Recent progress on smart hydrogels for biomedicine and bioelectronics. *Biosurface Biotribol*. 2022; 8(3): 212-24. <https://doi.org/10.1049/bsb2.12046>
15. Aktas N, Alpaslan D, Dudu TE. Polymeric organo-hydrogels: novel biomaterials for medical, pharmaceutical, and drug delivery platforms. *Front Mater*. 2022; 9: 845700. <https://doi.org/10.3389/fmats.2022.845700>
16. Xiao Y, Wang ZY, Luo SH, Lin JY, Cao XY, Fang YG. One-pot preparation of thermosensitive poly(lactic acid) materials by modifying with N-Isopropyl acrylamide. *Polymer*. 2021; 231: 124126. <https://doi.org/10.1016/j.polymer.2021.124126>
17. Amiryaghoubi N, Fathi M, Pesyan NN, Samiei M, Barar J, Omidi Y. Bioactive polymeric scaffolds for osteogenic repair and bone regenerative medicine. *Med Res Rev*. 2020; 40(5): 1833-1870. <https://doi.org/10.1002/med.21672>
18. Bashir MH, Korany NS, Farag DB, Abbass MM, Ezzat BA, Hegazy RH, Dörfer CE, Fawzy El-Sayed KM. Polymeric nanocomposite hydrogel scaffolds in craniofacial bone regeneration: A comprehensive review. *Biomolecules*. 2023; 13(2): 205. <https://doi.org/10.3390/biom13020205>
19. Hu Y, Shin Y, Park S, Jeong JP, Kim Y, Jung S. Multifunctional Oxidized Succinoglycan/Poly (N-isopropylacrylamide-co-acrylamide) Hydrogels for Drug Delivery. *Polymers*. 2022; 15(1): 122. <https://doi.org/10.3390/polym15010122>
20. Arican F, Uzuner-Demir A, Sancakli A, Ismar E. Synthesis and characterization of superabsorbent hydrogels from waste bovine hair via keratin hydrolysate graft with acrylic acid (AA) and acrylamide (AAm). *Chem Pap*. 2021; 75: 6601-10. <https://doi.org/10.1007/s11696-021-01828-z>
21. Lysáková K, Hlinakova K, Kutalkova K, Chaloupková R, Zidek J. Novel approach in control release monitoring of protein-based bioactive substances from injectable PLGA-PEG-PLGA hydrogel. *Express Polym Lett*. 2022; 16(8): 798-811. <https://doi.org/10.3144/expresspolymlett.2022.59>
22. de Brito AE, Pessoa Jr A, Converti A, de Oliveira Rangel-Yagui C, da Silva JA, Apolinário AC. Poly (lactic-co-glycolic acid) nanospheres allow for high l-asparaginase encapsulation yield and activity. *Mater Sci Eng C*. 2019; 98: 524-34. <https://doi.org/10.1016/j.msec.2019.01.003>
23. Kongprayoon A, Ross G, Limpeanchob N, Mahasaranon S, Punyodom W, Topham PD, Ross S. Bio-derived and biocompatible poly (lactic acid)/silk sericin nanogels and their incorporation within poly (lactide-co-glycolide) electrospun nanofibers. *Polym Chem*. 2022; 13(22): 3343-3357. <https://doi.org/10.1039/D2PY00330A>
24. Munim SA, Raza ZA. Poly (lactic acid) based hydrogels: Formation, characteristics and biomedical applications. *J Porous Mater*. 2019; 26(3): 881-901. <https://doi.org/10.1007/s10934-018-0687-z>
25. Qamruzzaman M, Ahmed F, Mondal MIH. An overview on starch-based sustainable hydrogels: Potential applications and aspects. *J Polym Environ*. 2022; 30(1): 19-50. <https://doi.org/10.1007/s10924-021-02180-9>

26. Seow WY, Kandasamy K, Purnamawati K, Sun W, Hauser CA. Thin peptide hydrogel membranes suitable as scaffolds for engineering layered biostructures. *Acta Biomater.* 2019; 88: 293-300. <https://doi.org/10.1016/j.actbio.2019.02.001>
27. Allen R, Ivchenko E, Thuamsang B, Sangsuwan R, Lewis JS. Polymer-loaded hydrogels serve as depots for lactate and mimic “cold” tumor microenvironments. *Biomater Sci.* 2020; 8(21): 6056-68. <https://doi.org/10.1039/D0BM01196G>
28. Ghorbanizamani F, Moulahoum H, Celik EG, Timur S. Ionic liquids enhancement of hydrogels and impact on biosensing applications. *J Mol Liq.* 2022; 357: 119075. <https://doi.org/10.1016/j.molliq.2022.119075>
29. Kesharwani P, Bisht A, Alexander A, Dave V, Sharma S. Biomedical applications of hydrogels in drug delivery system: An update. *J Drug Deliv Sci Technol.* 2021; 66: 102914. <https://doi.org/10.1016/j.jddst.2021.102914>
30. Cao X, Liu H, Yang X, Tian J, Luo B, Liu M. Halloysite nanotubes@ polydopamine reinforced polyacrylamide-gelatin hydrogels with NIR light triggered shape memory and self-healing capability. *Compos Sci Technol.* 2020; 191: 108071. <https://doi.org/10.1016/j.compscitech.2020.108071>
31. Attia MF, Montaser AS, Arifuzzaman M, Pitz M, Jlassi K, Alexander-Bryant A, Kelly SS, Alexis F, Whitehead DC. In Situ Photopolymerization of Acrylamide Hydrogel to Coat Cellulose Acetate Nanofibers for Drug Delivery System. *Polymers.* 2021; 13(11): 1863. <https://doi.org/10.3390/polym13111863>
32. Chafran L, Carfagno A, Altalhi A, Bishop B. Green Hydrogel Synthesis: Emphasis on Proteomics and Polymer Particle-Protein Interaction. *Polymers.* 2022; 14(21): 4755. <https://doi.org/10.3390/polym14214755>
33. Dewangan Y, Verma DK, Berdimurodov E, Haldhar R, Dagdag O, Tripathi M, Mishra VK, Kumar PA. N-hydroxypyrazine-2-carboxamide as a new and green corrosion inhibitor for mild steel in acidic medium: experimental, surface morphological and theoretical approach. *J Adhes Sci Technol.* 2022: 1-21. <https://doi.org/10.1080/01694243.2022.2068884>
34. Berdimurodov E, Kholikov A, Akbarov K, Guo L, Kaya S, Kumar Verma D, Rbaa M, Dagdag O. Novel glycoluril pharmaceutically active compound as a green corrosion inhibitor for the oil and gas industry. *J Electroanal Chem.* 2022; 907: 116055. <https://doi.org/10.1016/J.JELECHEM.2022.116055>
35. Dagdag O, Haldhar R, Kim SC, Guo L, El Gouri M, Berdimurodov E, Hamed O, Jodeh S, Akpan ED, Ebenso EE. Recent progress in epoxy resins as corrosion inhibitors: design and performance. *J Adhes Sci Technol.* 2022: 1-22. <https://doi.org/10.1080/01694243.2022.2055347>
36. Berdimurodov E, Kholikov A, Akbarov K, Guo L, Kaya S, Katin KP, Verma DK, Rbaa M, Dagdag O, Haldhar R. Novel gossypol-indole modification as a green corrosion inhibitor for low-carbon steel in aggressive alkaline-saline solution. *Colloids Surf A Physicochem Eng Asp.* 2022; 637: 128207. <https://doi.org/10.1016/J.COLSURFA.2021.128207>
37. Berdimurodov E, Kholikov A, Akbarov K, Guo L. Inhibition properties of 4,5-dihydroxy-4,5-di-p-tolyimidazolidine-2-thione for use on carbon steel in an aggressive alkaline medium with chloride ions: Thermodynamic, electrochemical, surface and theoretical analyses. *J Mol Liq.* 2021; 327: 114813. <https://doi.org/https://doi.org/10.1016/j.molliq.2020.114813>

## بلمرة الأكريلاميد -N- ميثيلين اللاكتيك وحمض الجليكوليك

سفارا خازرتكلوفا<sup>1</sup>، نوديرا زوكيروفا<sup>1</sup>، بوسورا ميوخميدوفا<sup>1</sup>، باسانت لال<sup>2</sup>، اوريغون خميدوفا<sup>3</sup>، اليور بيردموردوفا<sup>4,5,6</sup>، كلوي عليفا<sup>6</sup>، احمد حسيني باندغاري<sup>7</sup>، نيزوميدين اليفا<sup>8</sup>

<sup>1</sup>كلية الصيدلة، معهد طشقند للصيدلة، طشقند، أوزبكستان.  
<sup>2</sup>قسم الكيمياء، معهد العلوم التطبيقية والعلوم الإنسانية، جامعة GLA، ماثورا-281406، الهند.  
<sup>3</sup>كلية التكنولوجيا الكيميائية، جامعة ولاية نافوي للتعليم والتكنولوجيا، نافوي، أوزبكستان.  
<sup>4</sup>الهندسة الكيميائية وهندسة المواد، جامعة أوزبكستان الجديدة، 1، شارع موفاروناهر، منطقة ميرزو أولوغبيك، طشقند، 100000، أوزبكستان.  
<sup>5</sup>كلية الطب، جامعة آسيا الوسطى، طشقند 111221، أوزبكستان.  
<sup>6</sup>كلية الكيمياء، جامعة أوزبكستان الوطنية، طشقند، 100034، أوزبكستان.  
<sup>7</sup>كلية الكيمياء، جامعة سمنان، سمنان، إيران.  
<sup>8</sup>جامعة طشقند الحكومية للاقتصاد، طشقند، 100066 أوزبكستان.

### الخلاصة

الهدف من الدراسة هو تصنيع بوليمرات جديدة) أكريلاميد -N- ميثيلين اللاكتيك وحمض الجليكوليك (المشتقة من أحماض الهيدروكسي الطبيعية من خلال البلمرة الجذرية لمادة الأكريلاميد المستبدلة بـ N ، لاستكشاف التحول الكيميائي لبولي أكريلاميد ، وللتحقق من بعض الخصائص الفيزيائية والكيميائية لمادة البولي أكريلاميد. البوليمرات الناتجة. بالإضافة إلى ذلك ، يهدف البحث إلى تحديد التطبيقات الواعدة لهذه البوليمرات. لتجميع البوليمرات المحبة للماء الحساسة لدرجة الحموضة. ومن ثم ، تم إنشاء أكريلاميدو-إن-ميثيلين جليكوليك وأحماض اللبنيك أكريلاميدو-إن-ميثيلين لأول مرة باستخدام أحماض الهيدروكسي الطبيعية كأساس. تم التعرف على هيكل هذه المونومرات المركبة من خلال التحليل الطيفي للأشعة تحت الحمراء وطرق التحليل الفيزيائية والكيميائية المختلفة. تمت دراسة حركية البلمرة الجذرية للأكريلاميدو -N- ميثيلين جليكوليك وأحماض اللبنيك أكريلاميدو -N- ميثيلين في المحاليل المائية. أثبتت الاختبارات البيولوجية التي أجريت على حمض اللاكتيك بولي أكريلاميدو-إن-ميثيلين إمكاناته كمحفز لنمو النبات.

**الكلمات المفتاحية:** بولي أكريلاميد. حمض اللاكتيك؛ حمض الجليكوليك؛ البلمرة. بوليمرات ماء حساسة لدرجة الحموضة.